UC San Diego

UC San Diego Electronic Theses and Dissertations

Title

Design of running-man, a bipedal robot

Permalink

https://escholarship.org/uc/item/11r612s9

Author

Chen, Jin

Publication Date

2011

Peer reviewed|Thesis/dissertation

University of California, San Diego

Design of running-man, a bipedal robot

A Thesis submitted in partial satisfaction of the requirements
for the degree Master of Science

in

Engineering Sciences (Mechanical Engineering)

by

Jin Chen

Committee in charge:

Professor Tom Bewley, Chair
Professor Prab Bandaru
Professor Mauricio de Oliveira

2011

The Thesis of Jin Chen is approved and it is acceptable in
quality and form for publication on microfilm and electronically:

_____

_____

_____

<div align="right">Chair</div>

University of California, San Diego
2011

To my parents and my brother,
whose supports of my education are ever so generous

TABLE OF CONTENTS

Chapter 1 Introduction

Chapter 2 Previous Robots that Hop and Run

Chapter 3 Motors and Springs

Chapter 4 Robot Mechanical Design

Chapter 5 Simulation, Control and Electronics

Chapter 6 Test Results, Summary and Future Work

References

Appendices

LIST OF FIGURES

LIST OF TABLES

ACKNOWLEDGEMENTS

ABSTRACT OF THE THESIS

Design of running-man, a bipedal robot

by

Jin Chen

Master of Science in Engineering Sciences (Mechanical Engineering)

University of California, San Diego, 2011

Professor Tom Bewley, Chair

This thesis presents the design of the running man robot. The primary motivation behind the work is to create a platform for research into bipedal running motion. Running robots have been built before, but most of them relied on the sheer power of actuators-electric motors, pneumatic motors, and hydraulic motors. This thesis details a design of hopping robot that incorporates electric motors, torsion springs and extension springs. Torsion springs are mounted in parallel to the motor control. To improve the functionality of robot as a hopping test-bed, each torsion spring was designed with controllable bias.

Furthermore, ankle of the robot was designed for better storing kinetic energy while minimizing vibration.

The robot was designed to mimic the hopping and running gaits of human and animal in planner motion. Ideas of self balancing was thought to be possible but was not incorporated in time.

Chapter 1

Introduction

1.1 Goal of the Thesis

The goal of this research project was to design a freestanding bipedal robot that is able to hop and run. The main goal of the biped, the running-man, is to be a test system for the ensuring control research projects. The hopping/running mechanism is meant to emulate the behaviors of bipedal animals, such as bunnies, kangaroo and humans. The highlights of this robot, which defer itself from other previous robots are the following:

- It incorporates torsion springs at hip and knee joints to store kinetic energy during landing.

- It incorporates nonlinear springs at ankle/foot to further store kinetic energy and maximize hopping height.

- This robot is about the size of a small dog. Small enough to require little space for testing, and big enough to conduct obstacle avoidance experiments.

- This robot uses RC servos, which are cheap to replace and easier to program than common DC servomotors, and have build-in gear reduction.

This thesis focuses on documenting the mechanical portion of the project. The design of the robot has been guided by several general goals, which include 3-lb overall weight, hopping on single foot, on both feet, and on alternating feet (running gait), and self-balancing.

The following points dominated the design decisions of the robots.

1. **Lightweight** The robot frame is made of aluminum 6061-T6. It was so chosen because its versatility as structure member. To reduce weight, unnecessary materials are removed using milling process so that only truss members remained to maintain structure strength. In general, a wall thickness of .05"-.06" is maintained throughout. Besides aluminum, there are some shafts that are made of stainless steel for a higher hardness. These shafts are generally hollowed out in order to lose weight. A lighter weight is critical to achieve higher hopping height and extend battery run time.

2. **Torsion springs** A torsion spring is seated at each joint. Springs absorb energy when hips and knees joints bends.

3. **RC servo motors** RC servos are the "muscles" of the robot. Two types of RC servo motors are used. High speed, low torque motors are suitable for directly rotating legs. Low speed, high torque motors are used to change torsion spring bias.

4. **Nonlinear spring foot** A non-linear spring is installed at the foot. It consists of a lever pulled by a linear extension spring. The lever is powering the up and down movements of rubber footpad. As the foot is pushed to up, it experiences a higher force and lower speed at beginning and a higher speed and a lower force at the end.

This robot is based on a previous robot of similar configuration made by a group of undergraduates. The major features of the current robot design is similar. That previous robot suffers various shortcomings, which prevent it from performing

jumping or hopping motion. Mechanically the major improvements from the previous robots are: added torsion springs, added ankles, improved stiffness of thighs and shins, and ball-bearing joints.

1.2   Summary of the Thesis

This thesis presents the design of the running-man robot

- Chapter 2 describes previous hopping and running robots.

- Chapter 3 describes the motors and the springs.

- Chapter 4 describes the mechanical specifics of the robot.

- Chapter 5 describes the electronics, sensor, computer simulation and control systems on the robot.

- Chapter 6 presents the results of research, some conclusions, and some points for future developments.

Chapter 2

Previous Robots that Hop and Run

2.1 Hopping Mechanism

Legged locomotion has the advantage of able to transverse through stairs, steps, crevices and rough terrains. Moving with legs for a robot is a desirable method locomotion because legged robots will have a greater access to the environments frequently visited by human as such apartment buildings and hiking trails and also to the environments hazardous to human such as lava fields, a contaminated nuclear plant, and battle fields. Simple walking gait can be performed relatively easily but walking is slow so it has limited applications. In order to speed up the movement of a robot, it's important to implement hopping and running gaits into a robot, with the hopping gait as a precursor of running gait.

To perform the running gait using only actuator is expensive. In order to lift the body to a height of h, minimum energy requires is given by mgh, where m is the mass of body, and g is gravity. Animals perform this feat by having spring-like bodies that capture some of the energy from previous jump to rebound, so it's only nature for robots to use a similar mechanism. By having springs in the legs, a robot can store kinetic energy from one jump and use it on the next.

Springs have been incorporated into previous robot designs. There are two categories of design that can be distinguished by the type of actuators employed. One uses hydraulic or pneumatic actuators, and the other uses electric motors. The

hydraulic actuators can be controlled to absorb energy by shutting off the valve before the foot hit the ground, such as a pogo stick. Therefore this design does not require additional a spring at each joint in addition to a actuator. On the other hand, electric motors can't be run like spring. So a design with electric motors must incorporate springs at the joints.

2.2 Previous Hopping Robots

In 1984, Raibert developed a one-leg hopper [1] that has hydraulic actuators and a telescoping leg with a pneumatic spring. The hopper moved stably along the plane. Later he was able to develop 2-leg hopper that stabilized in 3D using the same concept.
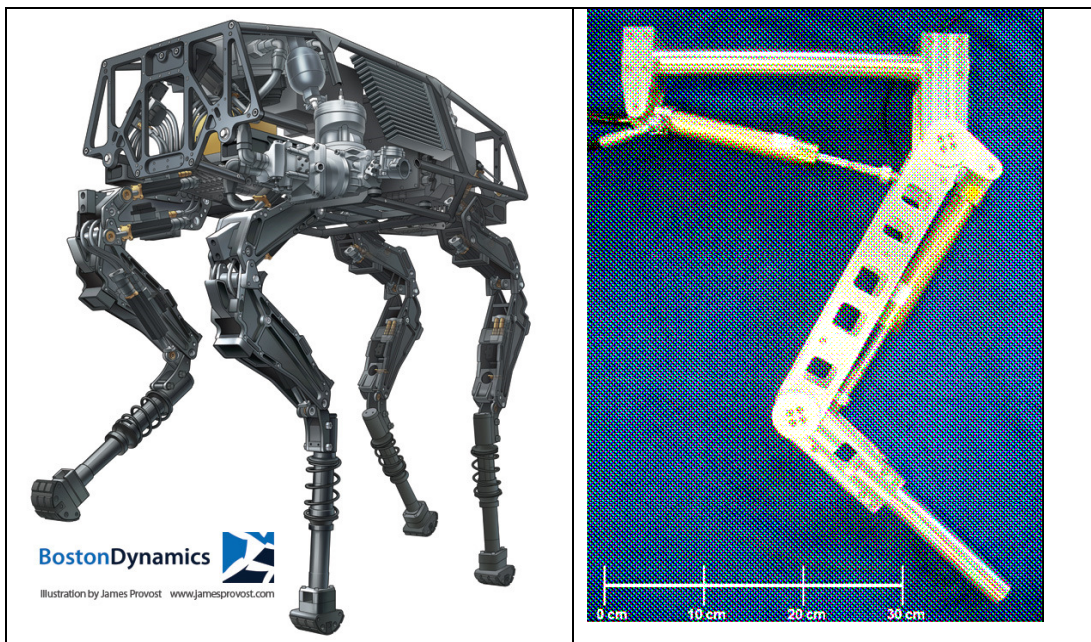
Figure 2.1 Big dog robot by Boston Dynamics(left) and leg of HyQ robot (right)

Two recent successful examples using hydraulic motors are the Big Dog robot made by Boston Dynamics[2] and Hydraulically Actuated Quadruped (HyQ)[3] made by Italian Institute of Technology. Both robot designs use hydraulic linear actuators to power the legs. Hydraulic linear actuators have high power to weight

ratio and higher speed of response comparing to electric motors. Hydraulic cylinders can also partially absorb the kinetic energy of hopping. A robot with hydraulic appendage can easy lift its own weight with ample spare power left for control. So that performing gaits like hopping and running is a relatively easy task.
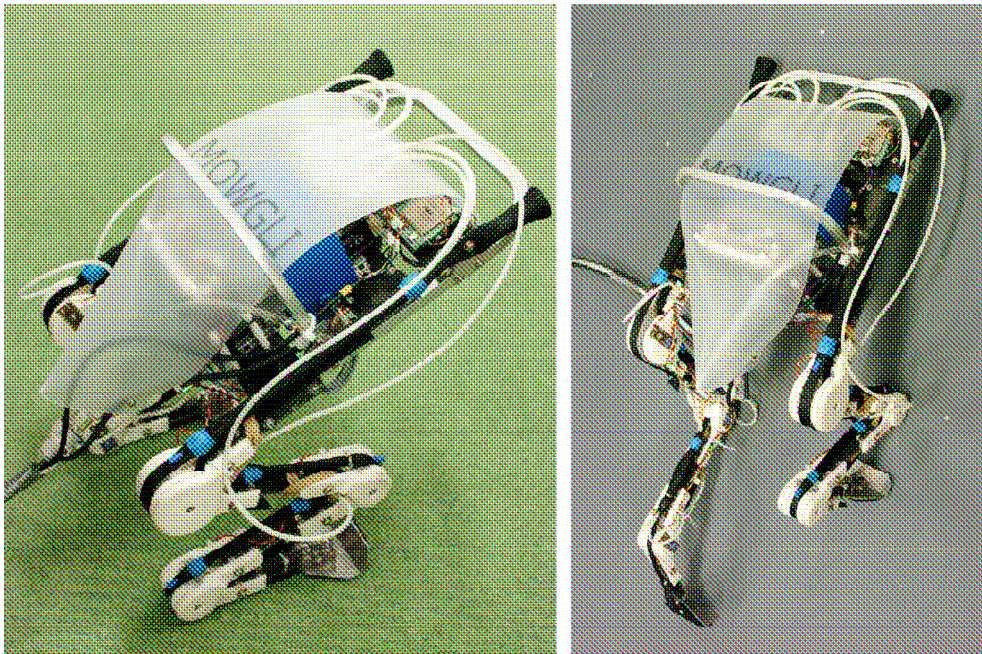
Figure 2.2 Jumping and landing robot Mowgli.

Mowgli[4] is a frog-like robot with pneumatic artificial musculoskeletal system and 6 degree of freedom. The robot is capable of impressive jumping feat. It can jump up ½ of body height, or the height of an office chair.

However hydraulic and pneumatic actuators suffer the problem that force and velocity responses are nonlinear so that these systems are hard to model and control. Additionally power storage is another problem with these actuators. A hydraulic system will require a fluid compressor, a reservoir/accumulator and an array of batteries.

Compare to hydraulic motors, electric motors suffer the disadvantages of having lower power density, lower torque at higher rpm (or for a higher torque, lower the rpm). In addition, modifying rotational motion into linear motion requires expensive and heavy ball screws and guides. To overcome these shortcomings of electric motors, engineers must design gear reductions, select appropriate springs, and optimize the robot kinematics, kinetics and control to achieve desirable results.

But electric motors have the advantages of more portable and scalable because they can draw power from batteries instead of compressors. Electric motors are also favored for precise positioning control, resulting increased stability. They also introduce less noise, and are often more available and affordable. It's these favorable characteristics that attract us to produce small robots using electric motors.

I-hops are a series of hopping robots developed by Chris M. Schmidt-Wetekam of UCSD. The figure below shows version 2 of I-hop, which uses a four-
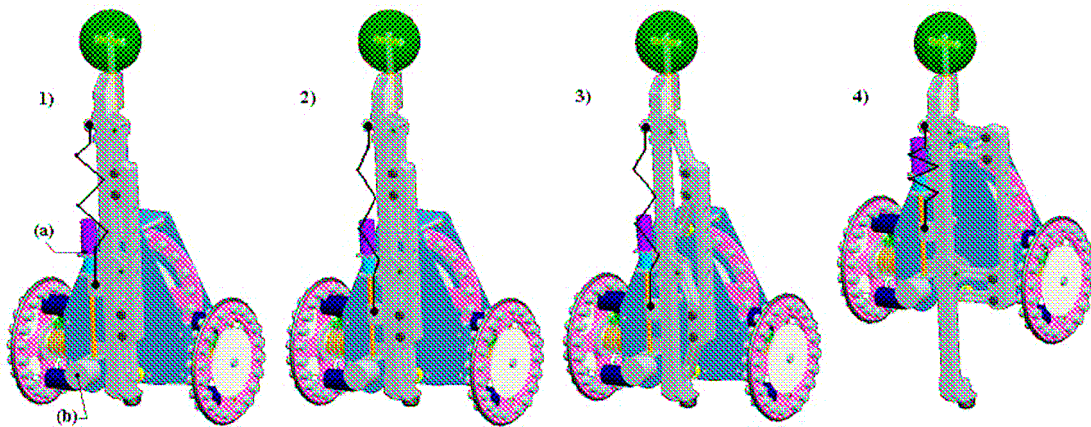
Figure 2.3 I-hop V2 developled by Chris M. Schmidt-Wetekam. Figure here is showing the "On-demand" hopping sequence.

bar linkage mechanism to maximize the take-off velocity of the robot. The robot hops by pulling the body upward with the tension springs and with the 4-bar linkages as its guide. As the 4-bar linkages turn from –90 degree to 0 degree, because of its kinematics, the vertical velocity is at its max.
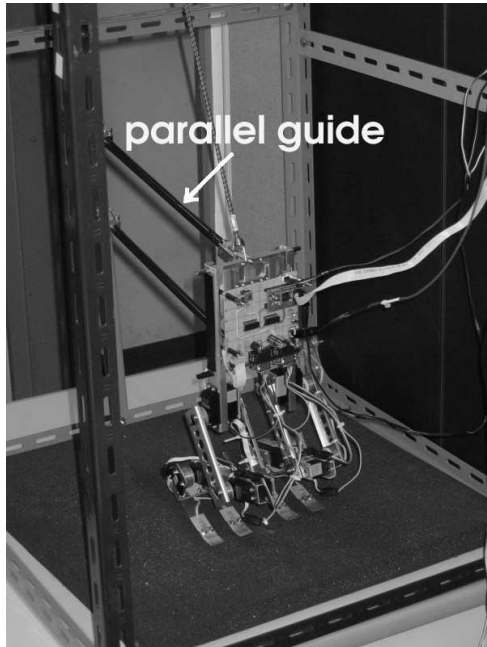
Figure 2.4 Unnamed robot by Meyer, Sproewitz, and Berthouze.

Another robot by Meyer, Sproewitz, and Berthouze[5] used RC servos to demonstrate a simple bipedal robot design. Flexible feet were installed to capture some of the kinetic energy between jumps. Their paper successfully compared the experimental data with a Lagrangian analytical study of the system. The authors also mentioned the problem of backlash that needs to be compensated with better control algorithm or additional force sensors.

OLIE (One Leg Is Enough)[6] is another robot developed by Department of Mechanical Engineering in Vrije Universiteit Brussel. The robot features only one leg

with two actuated joints (hip and knee). Power by two blushless motors and using timing belts to perform the necessary gear reduction, the robot also features horizontal beam acting as a torso to balance the robot in sagittal plane.
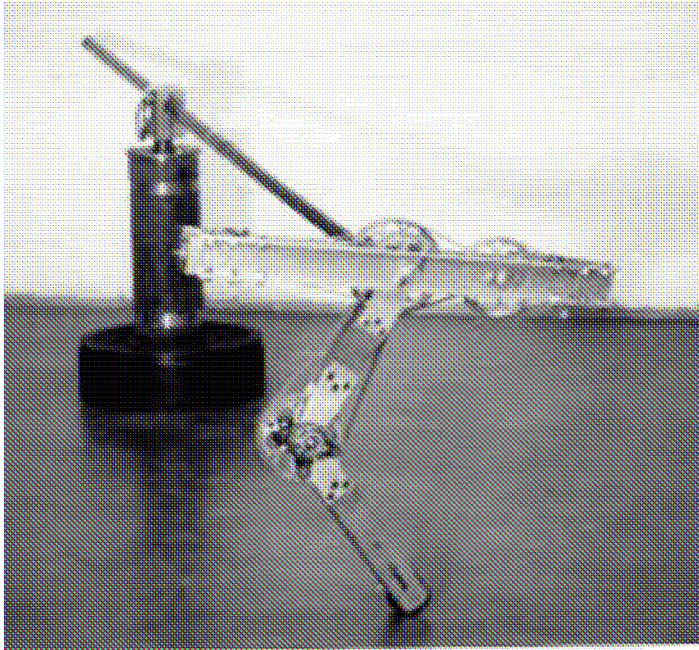
Figure 2.5   OLIE (One Leg Is Enough) seen in action.

For the running man project, the goal is set to explore a suitable design that will eventually result an autonomous robot that can perform human-like feats, such as walk, jump, and run. It would be a bipedal robot with each leg consists of a thigh, a shin and a foot. Actuators drive the thighs and the shins from hip and knee joints. The choice of selecting the lightweight RC servos as primary actuators is based on the following factors: 1. cost; 2. weight; 3 time. A RC servo is a more economic choice than a gear-head DC/AC servomotor. Each RC servo is packed with high gear reduction into an affordable package. Commercial gear head motor would cost probably 10 times more. With a on-board sensor and a motor controller, a RC servo

also reduces the cost of having a motor controller. A RC servo is also much lighter.

The built-in controller board has a very lightweight compared to commercial boards.

By having the on-board controller, a RC servo also helps eliminate some design and

programming tasks from users.

Chapter 3

Motors and Springs

This chapter describes the physical characteristics of the motor and springs used in the robot.

3.1 RC Servos

RC servos are cheap to buy and operate, easy to mount, and have a high ratio of holding torque to weight, therefore they are chosen as actuators of running-man.

HD DS120M

Drive motors for the legs are RC servomotors HD model DS120M. This motor was chosen because of the high rotation speed suitable for hopping application. DS-120M is fast digital metal gear servomotor. It is can operate on a voltage of up to 7.4v. Operating at 6V, it has a stall torque of 12.8 kg-cm(178oz-in) and the rotor can turn at a speed of 0.11 sec/60°. Range of movement is 0- 200 degree. The positional sensor inside the motor is a potentiometer. The motor weights only 56g so that torque to weight is considerably high.

Figure 3.1 Digital servo HD DS120M with metal gears (left) is the driver motor of the running man robot prototype and the smaller Hitec HS-55(right) is used to control torsion spring bias.

In the original configuration, only positioning control can be achieved. Changing the position requires a 5-7.6V pulse ranging from 1 to 2ms (see figure 3.2) [7]. With 1.5 ms pulse, the rotating arm is positioned to the middle of the range. The on-board motor controller is a feedback control with a 5K potentiometer as its sole sensor. So if the controller wants to rotate the arm to the middle of the range, it will read the voltage coming from potentiometer to decide its position and how far it has to turn.

Positioning control is not a desirable way of motor control for our robot, so that the motors have been modified to be controlled the micro controller instead. The details of the motor modification and controller design are described in Chapter 5.
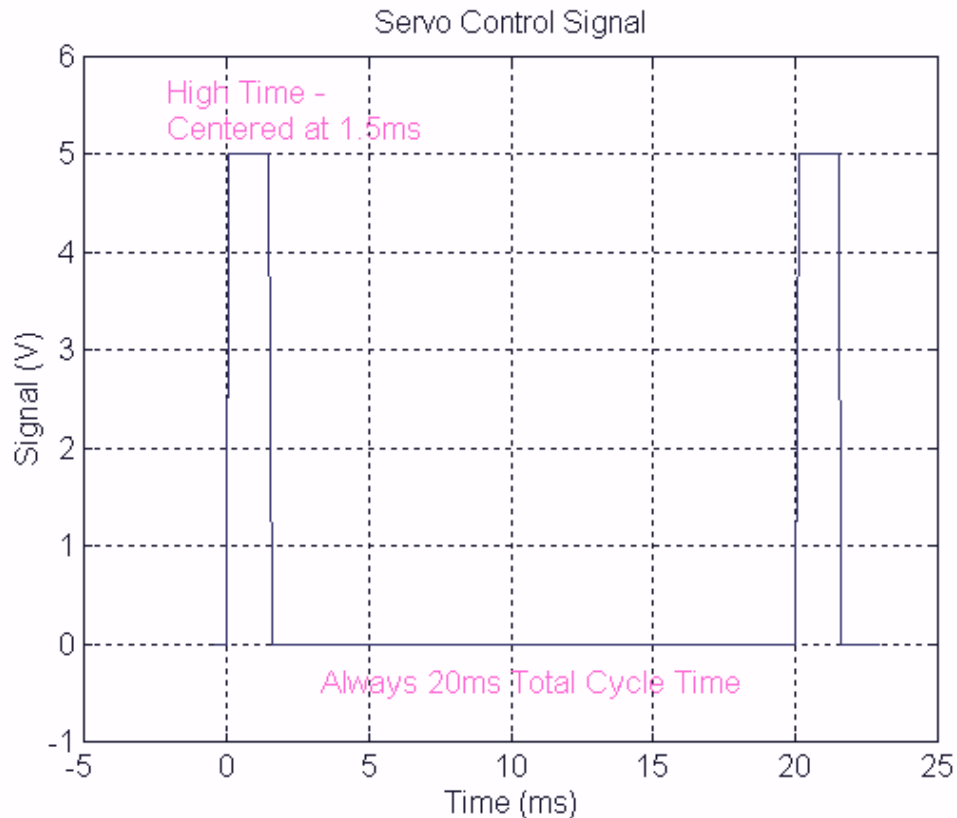
Figure 3.2 RC servo control signal

Hitec HS-55 Sub-micro servo

Beside drive motors, 4 servos are used to control the bias of torsion springs. The smaller, lighter, and less powerful HS-55 servos are used. This motor was chosen also because it can be hacked to operate continuously. It can operate on a voltage of up to 6V. Operating at 6V, it has a stall torque of 1.3 kg-cm(18 oz-in) and the rotor can turn at a speed of 0.14 sec/60°. Range of movement is 0- 180 degree. The motor weights 8g.

The motor by itself does not have enough torque to achieve the torsion spring bias, that's why external gear trains are added. A 24:1 gear train is used at hip joint, and a 88:1 gear train is used at knee joint.

Original motor movement range of 0-180 degree is not sufficient enough so that there motors were all modified to have full 360 degree of rotational freedom. The modification of electronics on this motor is the same as that of HD DS120M motors.

3.2 Torsion springs

The reasons of choosing torsion spring over others is its simplicity and its price. Behavior of a torsion spring is linear, as $T = \tau\Theta$, and $Kp = \frac{1}{2}\tau\Theta^2$, where τ is the spring constant. Therefore it behavior can be easily estimated. It's also simple to mount a torsion spring at a joint. Using a linear spring would require additional components or the behavior will lost its linearity.

Music wire torsion springs from McMaster are installed at hip and knee joints. Their properties are as follow: hip joint torsion spring $\tau =$ of 10.45 in.-lbs; knee joint torsion spring $\tau =$ 20.97 in- lbs. Selection of springs will be further discussed in Chapter 4.

Chapter 4

Robot Mechanical Design

This chapter presents the design specifics of the bipedal robot running man.

4.1. Legacy Design

Current design of running man can trace its root back to a previous design created by a group of undergraduate students, as shown in the figure below. Current design inherited the basic forms of torso, hip and knee. The body of that robot was acrylic. In order to scavenge the black RC servos shown in the figure for the running-man, that robot was disassembled at the beginning of the project.
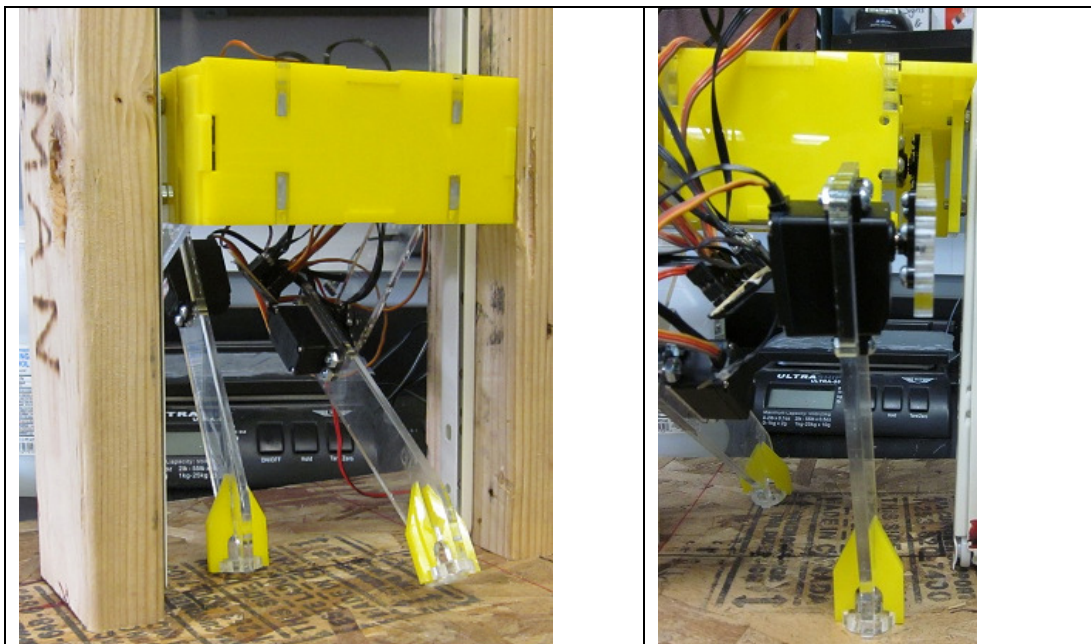
Figure 4.1 Running man legacy design. Left figure shows robot on a test stand. Right figure shows the details of right knee joint.

4.2. Design Overview

The running man consists of a body and two symmetrical legs. The body is made up of a horizontal beam, flanked by two triangular hips and with a cage-like box hanging beneath the horizontal beam. The hip is connected to the leg through a drive shaft. Drive motors are mounted on the body, which also houses the circuit board. Each leg is made up of thigh, shin and ankle. Thigh and shin are free to rotate. The ankle is fixed to the lower end of the shin. The foot is mounted to the ankle but the footpad can move up and down along a linear bearing.

Hip joint bearing and torsion spring housing

Circuit board housing

Thigh assembly with servos and gears controlling spring bias

Drive motors

Knee bearing and torsion spring housing

Ankle assembly with lever, extension spring, and foot shaft

Visco-elastic rubber foot
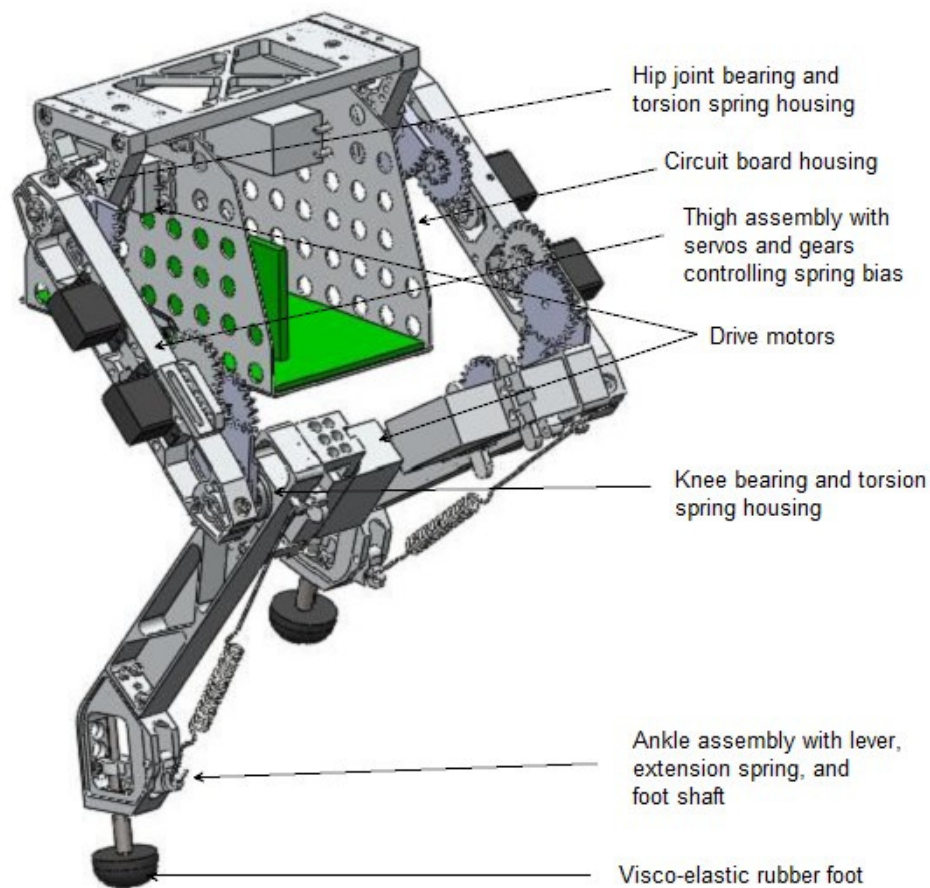
Figure 4.2 CAD model of the leg prototype with caption of the main mechanical features.

The robot can stand up to 1.2 feet when it erects. It weighs 2.3 pound without the battery. With reference to the body, the robot has 4 degrees of rotational freedom.

Four identical RC servos are used to power the leg at both hip and knee joints. Two different torsion springs are used at hip and knee.
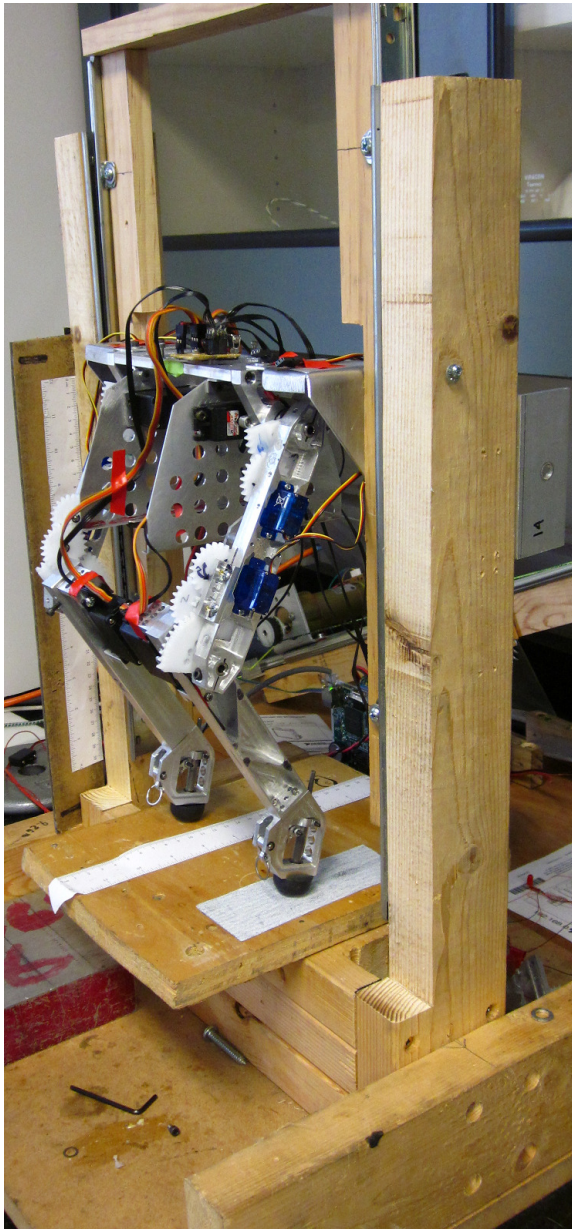
Figure 4.3 Actual picture of robot prototype fixed to a pair of vertical linear sliders.

In order to perform hopping and jumping experiments, a test bench as shown in Fig. 4.3 was developed, which allows the robot to move vertically up and down, guided by a pair of linear sliders. Coincidently the additional weight of the sliders

simulates the weight of the batteries that will be placed onboard. It's also possible to suspend the robot off the ground by fixing the slider at a certain height using a spacer block.
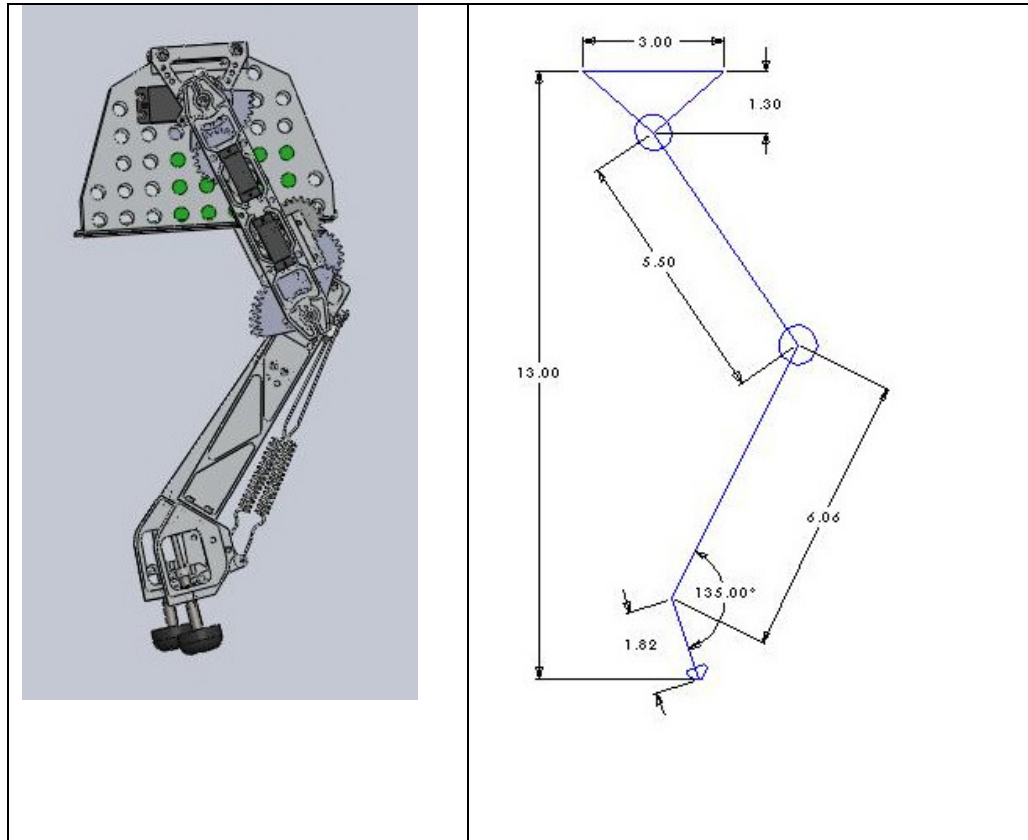
Figure 4.4 Side view of CAD model of the Running man prototype (left) and the sketch on the right showing dimensions between joints. Segments of legs are defined as follows: 1. hip; 2. thigh; 3. shin; 4. ankle.

Table 4.1 Specifications of Running Man robot prototype

Hip range of motion	0º - 90º
Knee joint range of motion	5º -100º
Thigh length	5.5 inches
Shin length	6.06 inches
Ankle-foot height (at rest)	1.8 inches

Rubber foot additional travel	.73 inches
Hip joint torsion spring	10.446 in.-lbs.
Knee joint torsion spring	20.97 in- lbs
Total weight (without batteries)	2.3 lbs
Weight of thigh sub-assembly	.2 lbs
Weight of shin-ankle-foot sub-assembly	.38 lbs

4.3. Selection of Torsion Springs

One important aspect of hopping gait is energy saving. In order to capture the kinetic energy of each jump, each leg of the robot contains three springs. Two of these are torsion springs, located separately at hip and knee joints.

Underlying theory

The goal of choosing appropricate springs is to maximize the input energy during "stance" (when the robot is standing on the ground). Since the energy stored in a torsion spring is given by $\frac{1}{2} \tau \Theta^2$, where τ is the angular stiffness and Θ is the bended angle. The energy storage is increased by stiffening the spring (increasing τ), But the amount of energy stored is more sensitive to the increase of total angular displacement Θ. For the same amount of potential energy, a stiff spring will have a larger τ, but smaller displacement; a soft spring will have a smaller τ, but larger displacement. The spring must at be able to support the weight of the robot by storing at least the same amount of energy as *mgh*, where h is the maximum vertical displacement of the robot's center of mass, m, above its lowest height during rebound.

There is an intrinsically undesired effect of configuring kinematics of our legs as running man or other bipedal animal. For a constant rotational velocity at knee and hip, the vertical velocity of end effecter, namely the center of mass, decreases as the leg extends during takeoff. The reason is the vertical velocity is proportional to cosine of linkage. As the angle increases from 0 to 90, the vertical velocity inevitably goes to zero. This effect is exactly the opposite of the desired effect.

The output vertical speed of the leg will be decreasing and goes to zero, which means that running-man will leave the ground before the leg becomes straight. As the leg extension velocity goes to zero, while the body continues to drift upwards.

Torsion springs are housed within the thigh and shin so they are concealed from plain view. It is so designed for both safety and aesthetic reasons. The spring housing also enclosed the bearing housing in its center.

4.4. Desired Leg Joints Kinematics

The kinematics side-view of running man shows the hip and the knee angles determine the position of the foot relative to the hip. For the convenience of implementing a simple control algorithm that makes the robot hop, we seek to keep the hip and the foot on the same vertical position, then the angles of hip and knee motor can be expressed using the following relationship:

$$\theta_k = \cos^{-1}(\cos\theta_h \bullet L_h / L_{shft}) + \theta_h - \theta_{ft}$$

	θ_h, θ_k Controlled by drive motors
	$L_h = 5.5"$
	$L_{sh} = 6.06"$
	$L_{shft} = 7.46"$
	$L_{ft} = 1.82"$
	$\theta_{ft} = 10°$
	$\theta_{ank} = 45°$
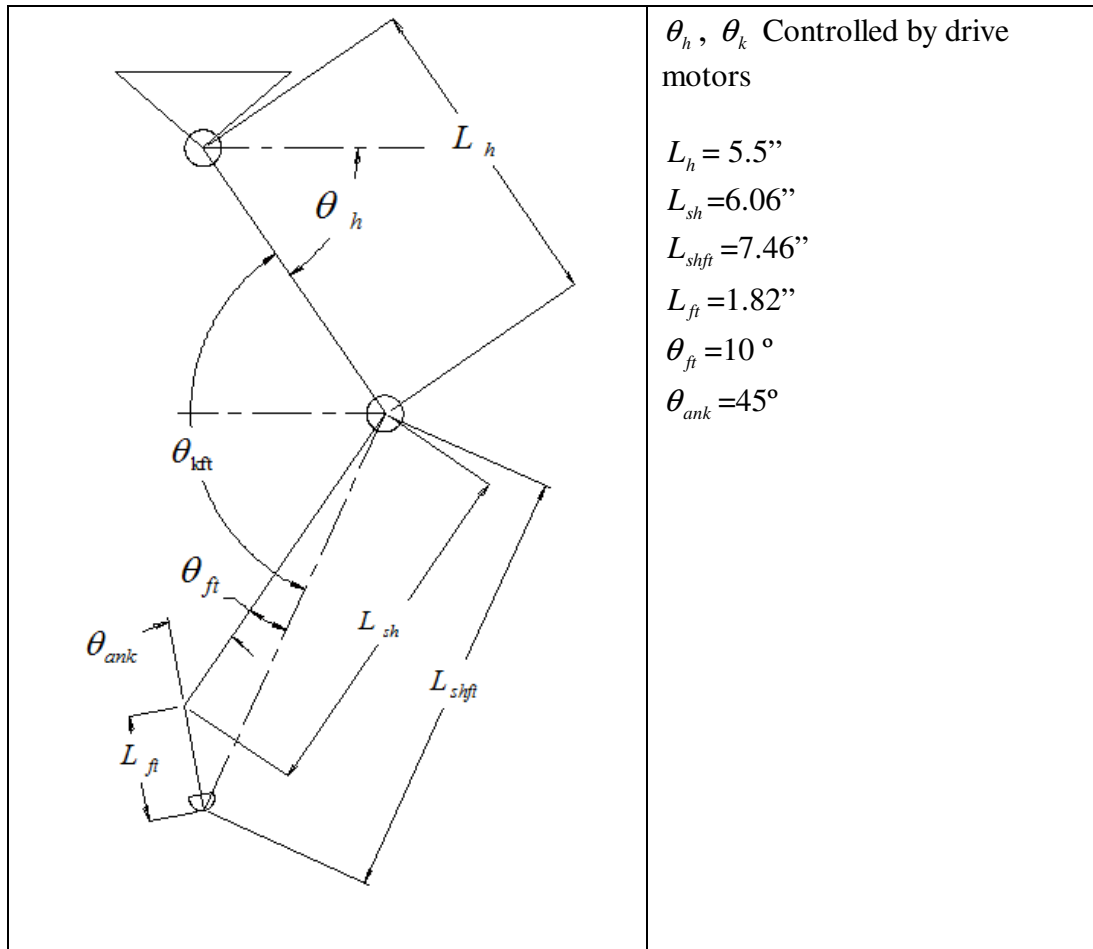
Figure 4.5 Kinematics of joints

4.5   Design of Ankle with Spring and Lever

Underlying theory

One important aspect of hopping gait is energy saving. An ideal hopping gait should efficiently capturing the kinetic energy as the foot lands on the ground and then releasing the energy when the foot bounces back up. For a legged robot, the amount of energy can be stored in the spring is important for achieving higher jumps, and saving energy expended by drive motor.

Many previous hopping robots have successfully used linear spring leg(s)/foot(feet) to achieve hopping and running. The robot made by Raibert, with pogo-stick leg, was simple yet efficient. The leg absorbs energy as the spring compressed by the foot. For a linear spring, the amount of potential energy stored is given by $E = \frac{1}{2}Kx^2$, with the spring force given by $F=Kx$. The energy can be stored is limited by the spring stiffness and spring compression

In practical use, there is a problem associated with the linear spring. In real life, a robot needs to be able to stand still as well as jump and hop. With a linear spring leg and reduced damping, the robot will inevitably wobble up and down even after motor power is cut off. Furthermore, energy stored in a linear spring has to be used immediately or will be lost. Therefore the simple linear spring design has the drawbacks when it comes to integrating with other robot gaits such as standing and walking.

To overcome the problem, the ankle is fitted with a simple nonlinear spring. The nonlinear spring consists a lever and an extension spring. One end of the lever is attached to the extension spring while the other end latched to a shaft, which in term acts on the foot. The torque created by the extension spring decreases as the foot moves upward because the perpendicular distance between the force and the fulcrum, decreases rapidly while spring force F_s only increase a little. On the other hand, the distance between the foot latch and the fulcrum, denoted as L, remains essentially the same. The result is the amount of force transferred from the extension spring onto the foot decreases gradually as the foot moves up. In our design, F_L is roughly inversely proportional the distance the foot travels. The spring exhibits the characteristics of

inverse spring constant, so the force can be expressed as $F_F = F_{F0} - K_F X$, where F_{F0} is the

pre-loading force. Energy stored in the spring is still expressed as $E = \frac{1}{2} K_F X^2$.

The ankle design helps stabilize the standing and walking gaits of robot, but

there are certain limitations with this design. The designed spring loading must never

exceed half of the body weight ($\frac{1}{2}mg$) so that the spring will compress with the robot

standing. Careful selection of extension spring and lever dimension is necessary to

make it work. This also means the amount of energy stored in the ankle will not be

able to lift the robot off the ground.
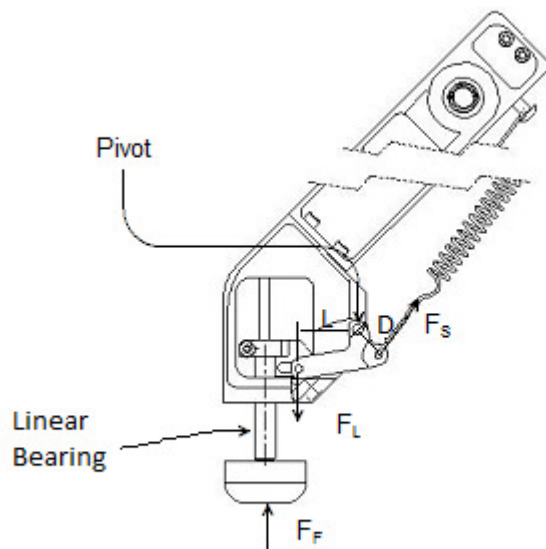
Figure 4.6 Design of an ankle with spring pulling a lever that actuates the up-and-down of foot.

Ankle Kinematics

The figure above shows the design detail of actual ankle mechanism.

Kinematics of lever is calculated under the assumption that friction is negligible

around the pivot. Then we have

$F_s·D=F_L·L$

If we can further assume that linear bearing is frictionless then

$F_L=F_F$

Therefore, we can estimate the maximum force the extension spring can have on the foot by

$F_F= F_s·D/L$

We selected a spring that has a constant of 1.6 lb per inch, and being preloaded to 2.1 lb initially.
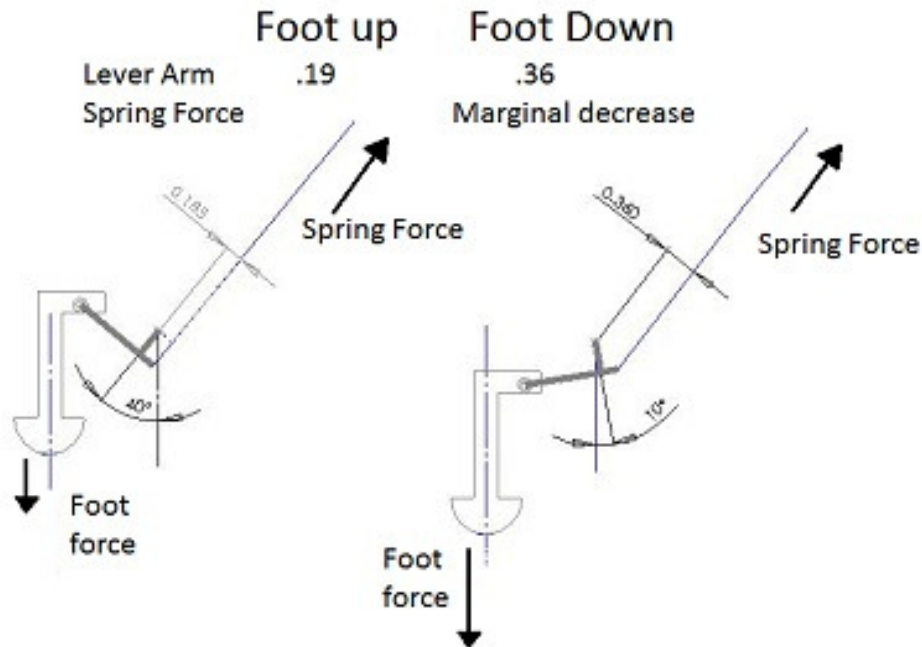
Figure 4.7 Figures shows the changes of lever dimension as the foot move down.
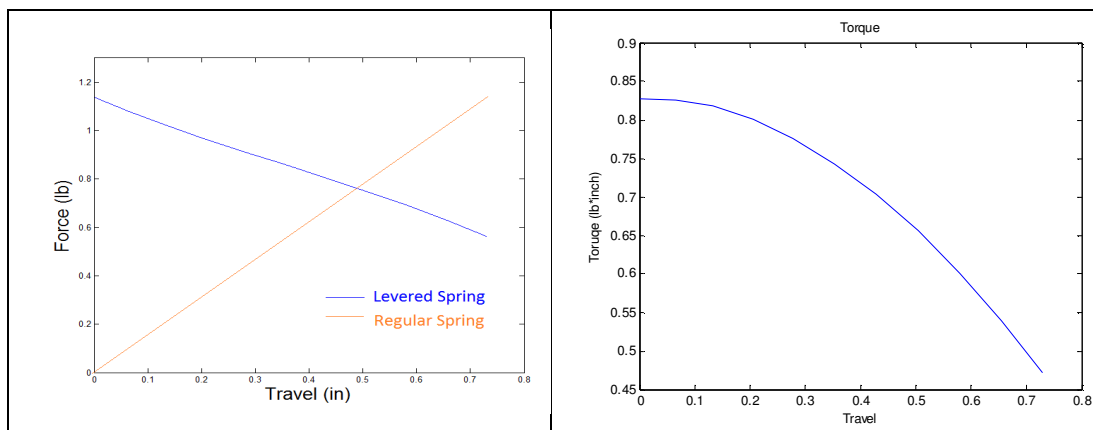
Figure 4.8 Figure left shows the force decreases as the foot is pushed upward. Right figure show the corresponding torque.

Using the dimensions and the forces given, a plot of the force verse distance shows that our spring has a maximum force of 1.15 lb. It decreases almost linearly as the foot is being pushed upward. Eventually it drops to .8 lb. The energy absorbed is about .74 inch-lb.

4.6   Design of Leaf Springy Foot
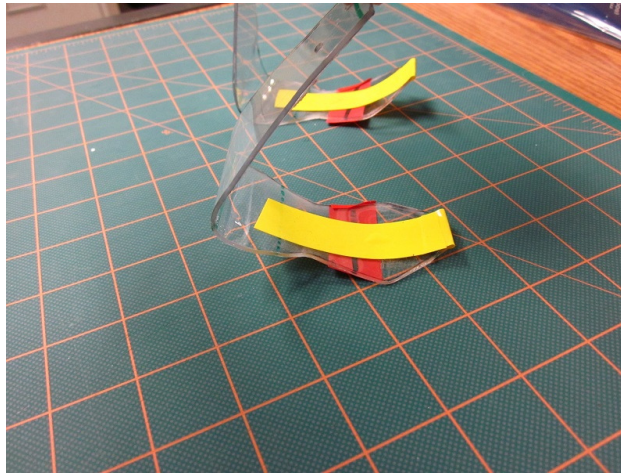
Figure 4.9 Picture of spring feet made of polycarbonate.

This is an offshoot from the main project with the hope of improving the jumping height of the robot. After testing with the ankle-foot, two areas of improvements were identified: 1, it weighs more than 48 gram, or about 1/30 of the robot total weight. But because it situated further away from the motors than the rest of the body, then having a lighter weight would make the control easier The lighter foot of the same energy capacity could in theory let the robot jump higher; 2, the efficiency of the shaft actuated foot decreases as the angle of touch down deviates from the upright direction. Therefore a possible alternative foot designs models after the flex prosthesis foot was designed and made. The design features a J shape body

with a curve foot bottom. For both convenience of the design and availability of

material, the new foot is made from polycarbonate sheet.

4.7   Torsion Spring Bias Mechanisms

Each of the torsion springs is fixed to variable bias mechanism on the hip and

knee joint where the springs are installed. The bias mechanism is made up of a micro

RC servo hitec55 driving a spur gear train. A 24:1 gear train is installed at the hip

joint and 88:1 gear train at the knee joint.
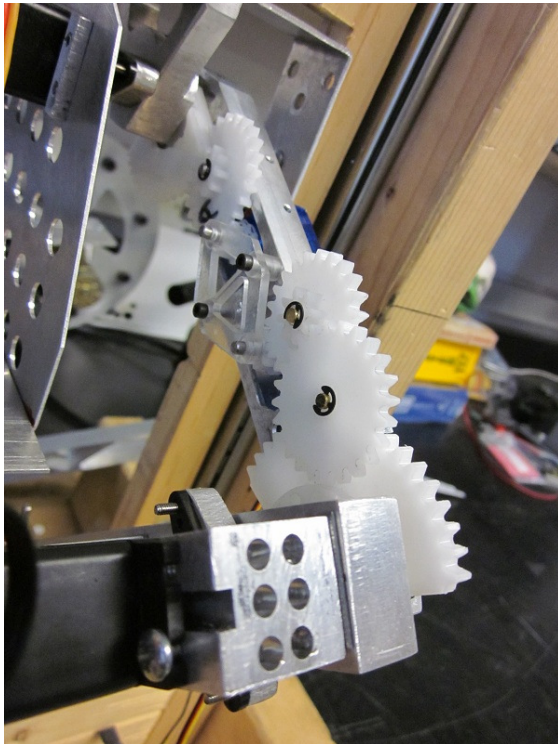
Figure 4.10 Photo of the gear train that controls the bias of right-knee torsion spring. Gears are machined delrin.

4.8 Weight and Friction Reduction

In order to maximize the overall mechanical efficiency of the hopping mechanism-in other words, minimize loss of energy in the process- special cares are taken toward reducing the weight of structure and minimizing friction at each joints.

Weight

Most of the weigh reduction is focused on the aluminum parts. Majority of the parts are made from aluminum 6061 for its good strength and good manufacturability. With the use of CNC milling machine in the lab, solid extrusion can be pocketed to thin wall. The thin structure is used on all major parts to retain structure stiffness and minimize weight. Truss bar is designed into body to further improve the strength of the component while keeping weight low. A .050-.055" thick wall is maintained through the design.

Other than aluminum body parts, drive shafts are made of stainless steel. They are hollowed through by drills to reduce weight.

Friction reduction with ball bearings

Ball bearings assemblies are used in each joint. It's feared that friction on the joints can take away much of the kinetic energy. Each bearing assemblies consists of two thin wall ball bearings pressed fit onto a bearing housing. Bearings are there to take on radial loads only, because axial loads are presumed to be small.

Unavoidable Friction within Servo Motors

There is an unavoidable present of friction within the gear train of each RC servo. The damping, coupled with inertia of gear train, reduce the efficiency of

energy absorption. As the condition of RC servos starts to deteriorate after some

testing, the efficiency is further reduced.

Chapter 5

Simulation, Control and Electronics

This chapter describes the Matlab simulations, the control algorithm and the electronics used in the robot.

5.1 Modeling and Simulation of Robot

Chris has developed the simulation and control of the robot. A Matlab and simulink simulation of running man has shown that stable running on the sagittal plane is possible with this design configuration. For the purpose of earlier experiment, a reduced version the simulation with only hopping mechanism is used to compare with experimental results.
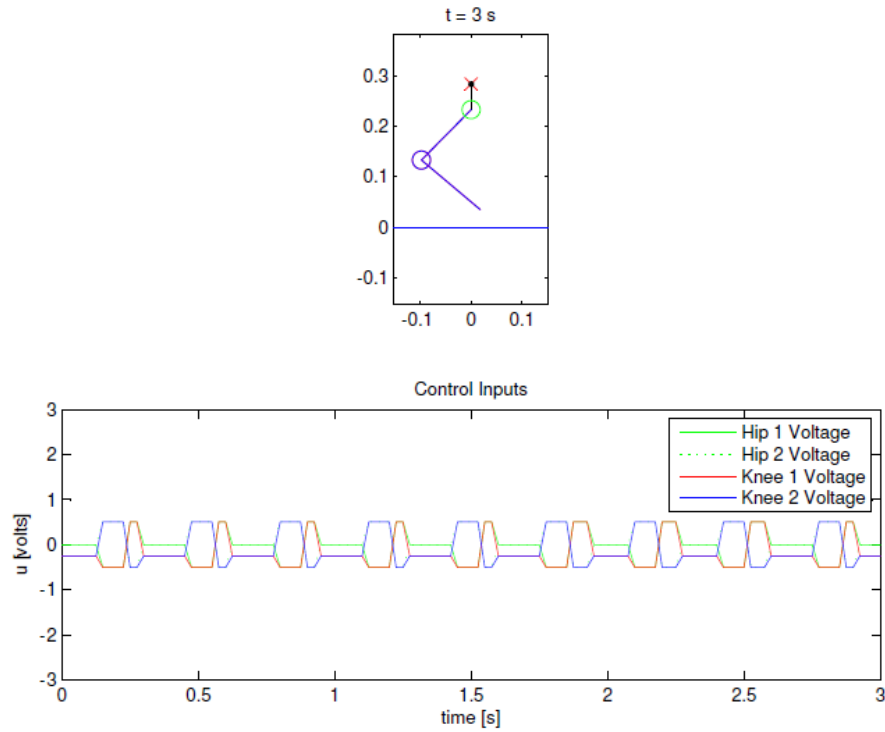
Figure 5.1 Simulation screen.

5.2 Electronics

In all our tests, a Single Board RIO (sbRIO) provide by National Instrument (NI) is used to interface with the robot. The board requires a 19V power supply to operate. It's connected to a computer through standard car5 cable. Chris did the setup of the board and the electronics.
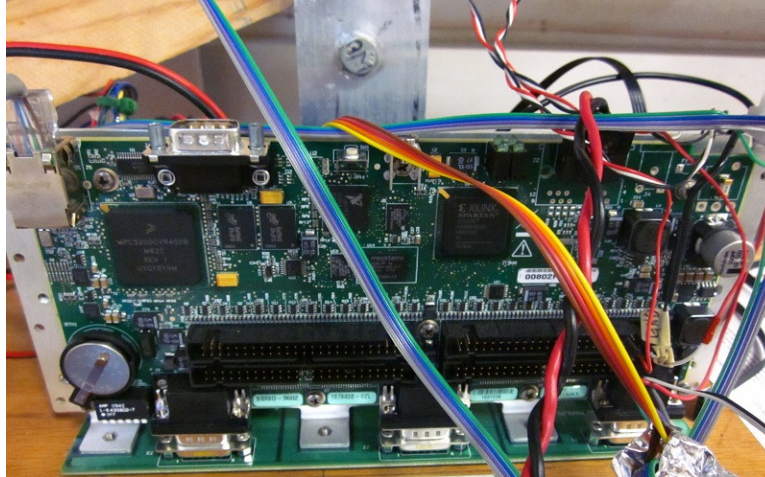
Figure 5.2 National Instrument sbRIO board.

What the sbRIO do in this project are reading the angle of each joint, and controlling the RC servos to actuate the hips and knees to desired angles. Each potentiometer within the RC servo provides us the necessary angle readings as a voltage between 0-5 volts. A 14-bit Analog to Digital (A/D) converter translates raw voltages to digital signals. The digital signals enable control of the motors done in the software.

In order to have real time reading from the joint angles, RC servos have been modified (see figure 5.3) and the control mechanism is modified. Originally the center terminal from the onboard 5k potentiometer goes to the on-board servo controller. That wire has been disconnected and the reading instead is fed into the A/D converter on SB-Rio. Onboard the RC servo, by using a voltage divider, a 2.5 V reference signal is sent to the original on-board controller so that the controller will always think the position is at 90 degree. The voltage divider in our cases is two identical surface-mount 2.4K resistors. This allows us to stop the servo with a string

of 1.5 ms pulses, or drive it proportionally forward or backward with pulses ranging

from 1 to 2 ms.
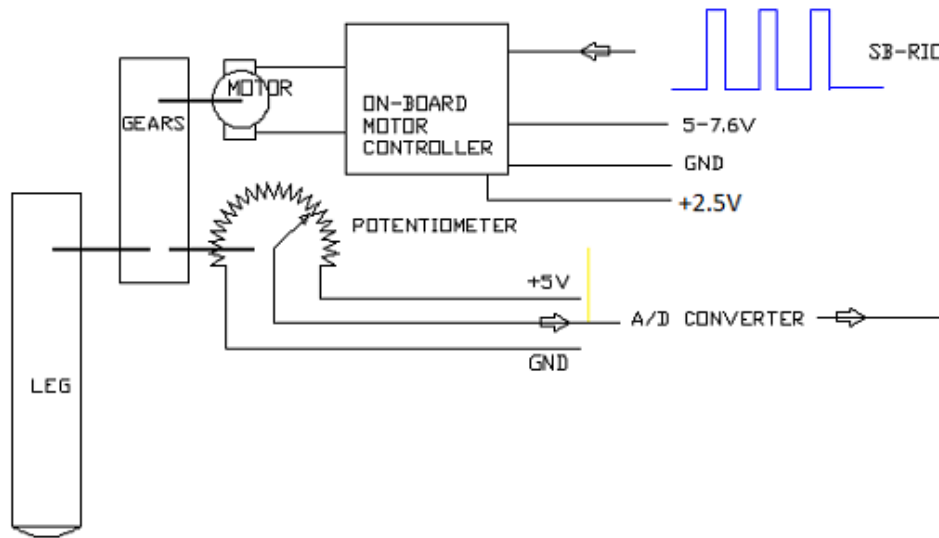
Figure 5.3 Motor control schematics.

5.3 Software Overview

For our experiments, the programming of the sbRIO was done within

Labview, also provided by NI. Labview interfaced with sbRIO seamlessly for most

part. Chris wrote the Labview program and the leg movement algorithm. I also

worked on some algorithm toward the later stage.

The Labview program with a Proportional Derivative (PD) controller is

implemented to perform the control of joints. The program takes the input readings

from potentiometers at each joint in term of a voltage between 0 V to 5 V, then runs

through some calculations and the instructions we have in algorithm, and then

determines the necessary output angles. At the end sbRIO board sends out the necessary Pulse Width Modulated signals to the on-board controllers of RC servo.

PD control is performed on the hip angle only. Essentially the knee joint motor is under an open-loop control, and the hip joint motor tries to match a PD-controlled angle based on knee angle. Since there is only position reading from potentiometers and no velocity sensing, rotational speed is estimated by the differential of angle within each sample time.

On the robot there is no external physical reference to angles the RC servos, so that the voltage readings from the joint angles have to be calibrated. Calibration was done by first positioning the robot to a chosen reference position and then match the voltage reading inside Labview to a decided reference voltage. For convenience purpose, an external reference position was selected at robot's upright posture with hip and knee angles at approximately 55 and 110 degrees, respectively. At this posture, foot and hip should line up vertically from a side view. A reference line on the test stand marks the height of the robot at that reference posture. In the Labview program, the amplitude window reads the voltage from potentiometers in real time (See figure 5.4). The voltage readings are marked by colors and a legend is provided. The procedure of the calibration goes as follows:

1.   Place the robot at the reference posture. The friction will generally keep it from moving. If not, hold it with spacer blocks.

2.   Inside the Labview, check to see if the voltages are at 2.5 V or not. If the reading from a joint is away from 2.5 V, loosen the clamping

screw at that joint and rotate the horn of RC servo until the voltage match to within 0.5V of 2.5 V.

3.   Tighten the joint clamping screw.
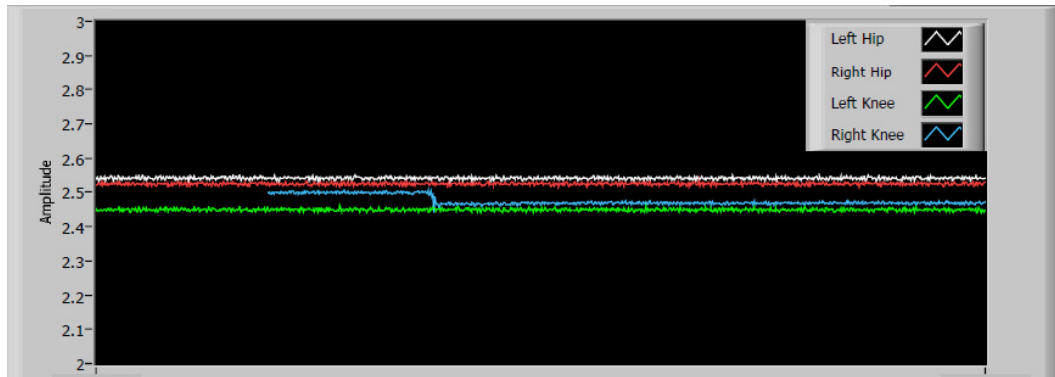
Figure 5.4 Calibration of potentiometer readings. The step in the blue line shows backlash of gears.

5.4 Hopping Algorithm Planning

The implementation of the hopping algorithm is done with a series of open loop commands. Previously Ryuma Niiyama had found that use of open loop system can "command a muscle-tendon mechanism to jump robustly". We were hopping that the same could be replicated here.

Challenges

In the course of implementing the control algorithm for the running man, it became evident that there were a few challenges associated with controlling the RC servos: noisy signals from potentiometers, limited bandwidth from the micro-controller to RC servo, and mechanical backlashes.

Position noise is less than 0.01 V, which is much less than the magnitude of actual positioning signal. For our purpose, this level of position noise is acceptable.

However velocity noise is much greater. The noise can spike to 1/10 of the actual signal, and that is because velocity is differentiated from the position so that noise from potentiometer is amplified in the process. A possible solution is to add velocity sensor such Gyroscope at each joint.

Servo response speed depends on the length cycle time. Micro controller sbRIO has limited computing power, which constraints the cycle time to.

Mechanical backlash seems to be the greatest cause of position inconsistency. The backlash within the gear train can range up to .03 V. That can translate to around 2 degrees of backlash, or about .3" off target.

Another problem is the on-board controller. Since originally the servo is not designed for the high rotational inertia, high speed condition, so the control experiences problem such as long settling time, and sometimes even instability. Since there is no way to reprogram the on-board controller, and the best solution is to tune the PD controller by trial and error.

Idealized Hopping Cycle

Each hopping cycle can be separated into 3 phases: compress, extend and flight. As the names imply, compress phase is when the leg compresses to store the energy; in the extend stage, the actuators push the apart to, and releasing the stored energy; after the robot leaves the ground, it is in flight state when it does nothing.
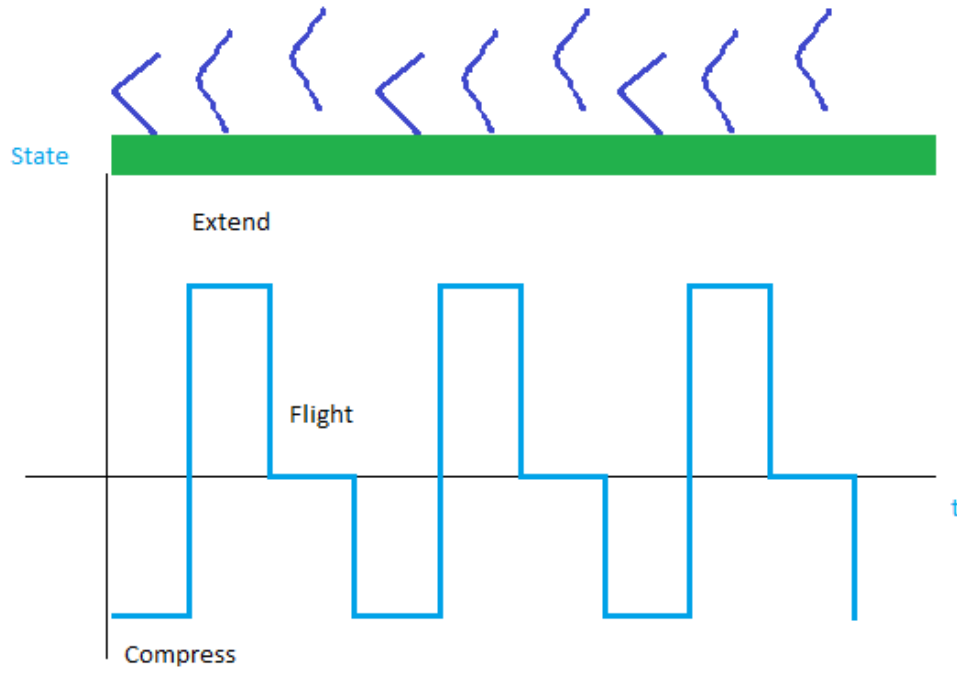
Figure 5.5 States of each hopping cycle starts compression when the robot leg is bent low to store the energy, then the leg is extended to push itself upward, eventual the robot is the air in the flight stages.

As previously discussed, the relationship between hip angle and knee angle

can be expressed by the following equation:

$$\theta_k = \cos^{-1}(\cos\theta_h \bullet L_h / L_{shft}) + \theta_h - \theta_{ft}$$

Ideally this equation should will be used determine the knee angle and achieve

synchronization of the two angles. However, the arcsine and cosine calculations are

calculation intensive and will take more time to run. To minimize the cycle time, a

linear equation was devised instead.

By plotting the two angles together and by plotting the differences between

these two angles, it was clear that the changes were comparably small over the range

of angles we are interested. In the initial implementations these differences were ignored- in other words, we assumed the two angles change at the same rate- in order to avoid intensive calculation and reduce the cycle time. The testing results were surprisingly stable and positive.

To further improve the result, a better relationship was developed by estimating rate of changes between two angles as linear. The figure below shows the relationship is almost linear. The following estimated relationship could be derived from the plot.

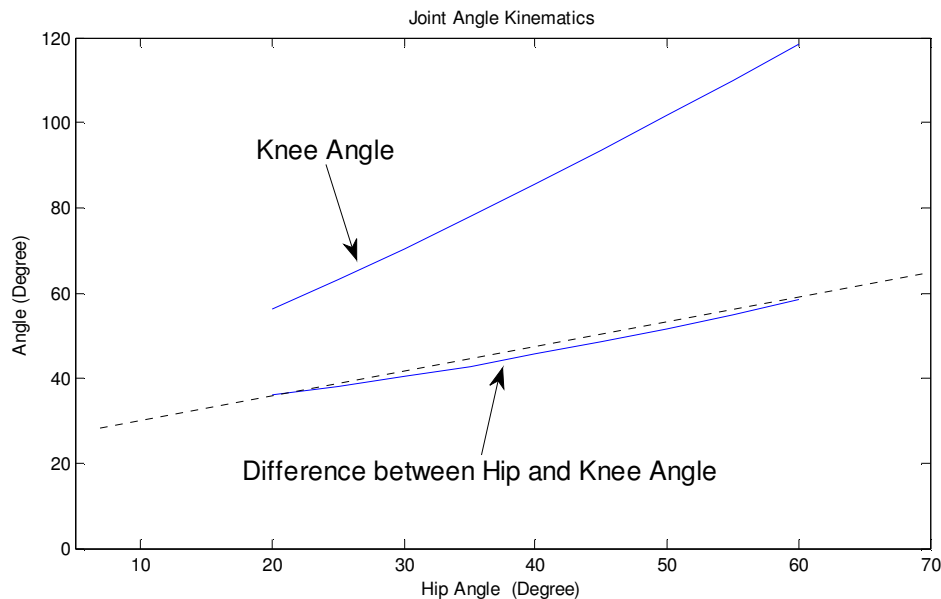$$\Delta\theta_{knee} \approx \frac{3}{2}\Delta\theta_{hip}$$

Figure 5.6 Difference in angles

The following table shows the voltage estimated from the linear equation derived above. The reference angles for the knee and hip are 110 and 55 degree, respectively.

Table 5.1 Estimated voltages as leg bends down

	Angle (Degree)	Voltage
Knee at standing posture	110	2.5 (Calibrated)
Knee at bend down posture	80	1.95 (Estimated)
Hip at standing posture	55	2.5 (Calibrated)
Hip at bend down posture	35	2.1 (Estimated)

$\Delta\theta_{hip} = 0°$
$\Delta\theta_{knee} = 0°$

$\Delta\theta_{hip} = 30°$
$\Delta\theta_{knee} = 50°$

Measured voltage in solid lines   Calculated voltage in doted lines
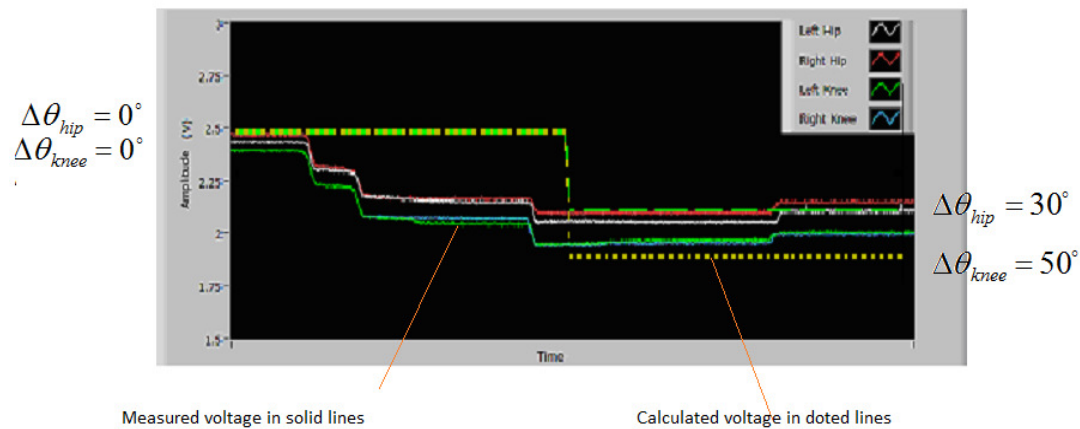
Figure 5.7 Plot of voltage during a calibration. Amplitude of 2.5 V marks the reference angle of both hip and knee angles, at 55 and 110 degree respectively. Voltages drop as the angles lower to 35 and 80 respectively.

Revisiting the desired kinematics issue, a plot of measured voltage vs. the calculated voltage is shown in Figure 5.6. There seems to be a little difference between the two sets of voltage, but the difference is small enough to have any major effect. Factors such as backlash and non-linearity in potentiometers might contribute to the differences.

5.5 PD Control Design

Inside the Labview, the PD controller is written in this form

$$\Delta\theta_{hip} = (0.67\Delta\theta_{knee} - \Delta\theta_{hip}) * Kp + (0.67\dot{\theta}_{knee} - \dot{\theta}_{hip}) * Kd$$

$\dot{\theta}_{knee}$ and $\dot{\theta}_{hip}$ are calculated using the following equation

$$\dot{\theta} \approx \frac{\Delta\theta - \Delta\theta_{old}}{timestep},$$

$\Delta\theta_{old}$ is the measurement from previous time step.

To find an approximate set of Kp and Kp for the controlling the hip angle, I simplified the complex dynamical system into a pendulum system with a straight bar hanging from the hip joint and the joint is actuated by the motor and the torsion spring. The

$$\begin{bmatrix} \dot{\theta} \\ \ddot{\theta} \end{bmatrix} = \begin{bmatrix} 0 & 1 \\ \dfrac{mgl - \tau}{I} & -b \end{bmatrix} \begin{bmatrix} \theta \\ \dot{\theta} \end{bmatrix} + \begin{bmatrix} 0 \\ \dfrac{a}{I} \end{bmatrix} V$$

$$T = aV - b\dot{\theta}$$

τ: the spring constant,

 l: length,

g: gravitational constant

V: voltage

T: Torque

Using the root locus plot, I was able to find a suitable PD controller with Kp=150 and Kd=10 that stabilize the system (see figure 5.7 and 5.8). The step response seems to have a steady-state error of 5%, but otherwise the controller has a

fast response and no overshoot. In the actual implementation of the controller, we
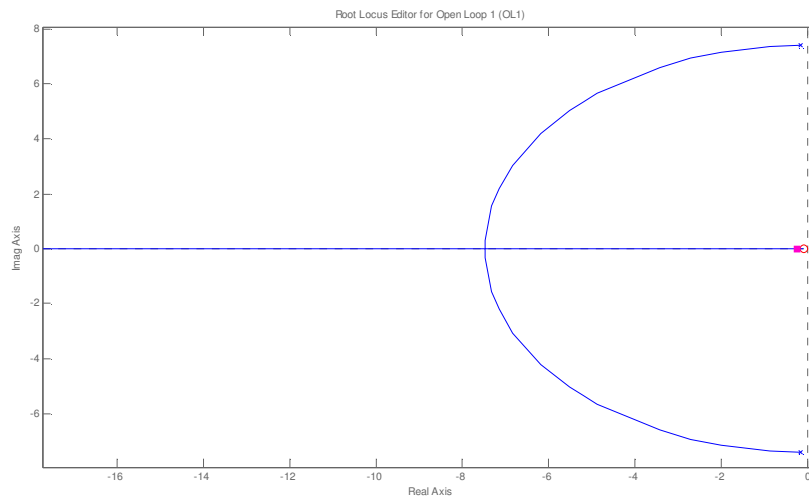
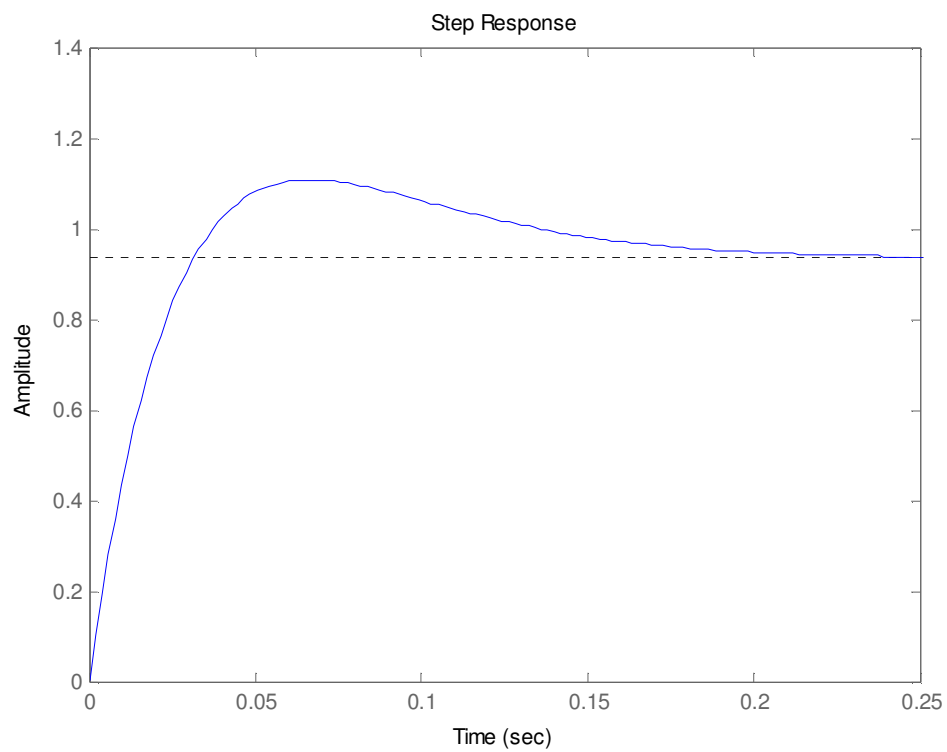scaled the gain, but maintained the ratio of Kp/Kd.

Figure 5.8 Root Locus plot

Figure 5.9 Step response of closed loop system.

Chapter 6

Test Results, Summary and Future Work

This chapter presents and discusses the results of the experiments, them summaries on the achievements and the problems, and makes recommendations for the future of the project.

6.1 Test on Hopping Gait

The implemented hopping algorithm is described as follow:

1. At extend stage; instruct both knee and hip motors to extend at maximum voltage to get the maximum lift.

2. After the robot takes off and enter the flight stage, the knee motors withdraw the shins as fast as possible in order to get the maximum ground clearance. The hip motors try to synchronize up hip angle with knee angle with a PD controller so the landing position is controllable.

3. After landing, all motors compresses at full speed in order to obtain the maximum compression angles.

Actual implementation of hopping goes by the following sequence:

Table 6.1 Hopping states

State	Knee	Hip
Extend	Extend shin	Extend thigh
Flight	Compress shin	PD control thigh to syn with shin
Compress	Compress shin	Compress shin

Loop

Data collected from hip and knee angle during a hopping sequence shows the control algorithm was successfully implemented.
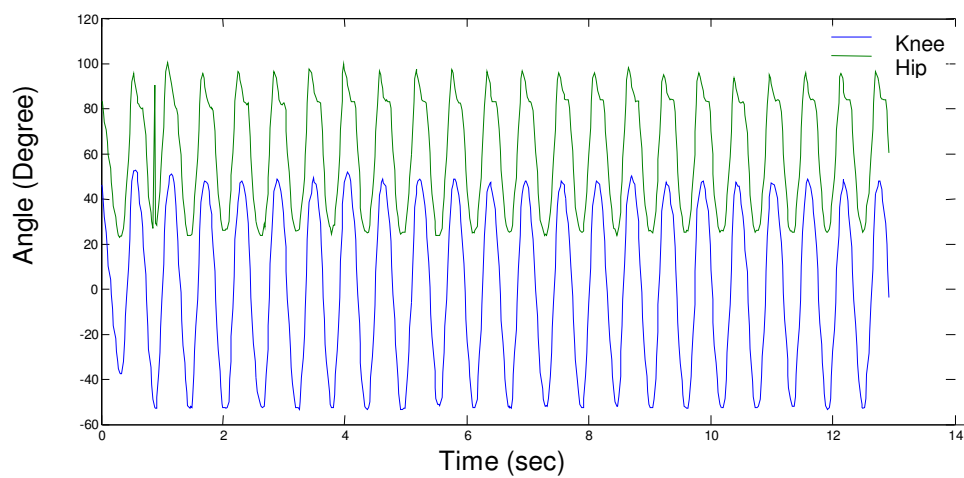

Figure 6.1 Test results showing hip angle and knee angles using hopping.
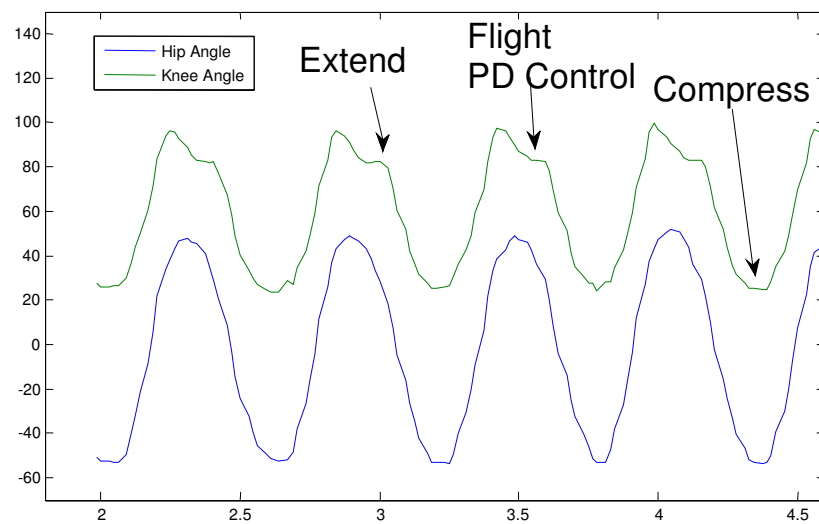

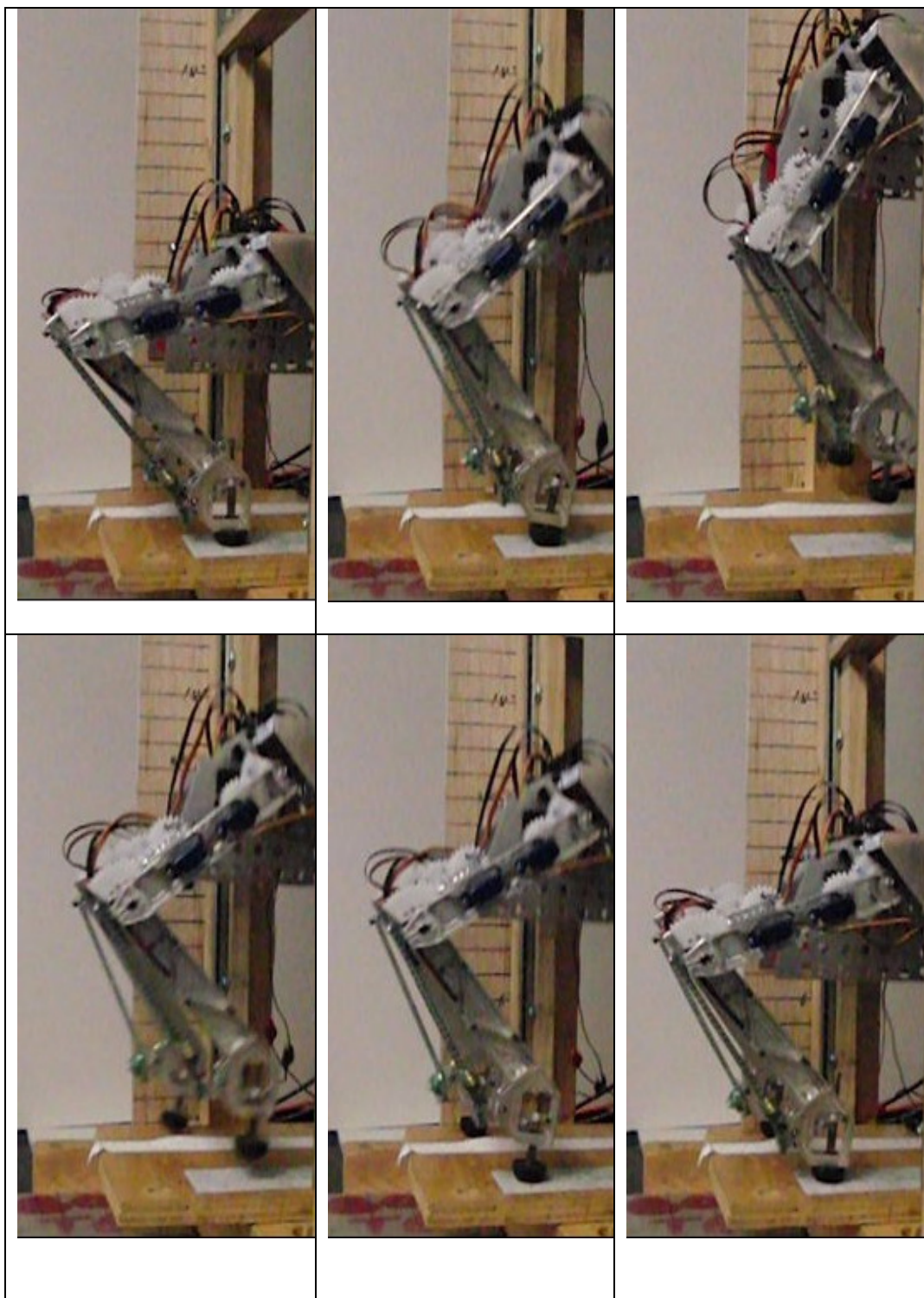**Figure 6.2 A zoom-in from previous plot.**

Figure 6.3 Figure shows the sequence of a complete jump. First two show the robot in extension phase, the next two show robot in flight, and the last two show the robot compressing.

Positioning of the Feet
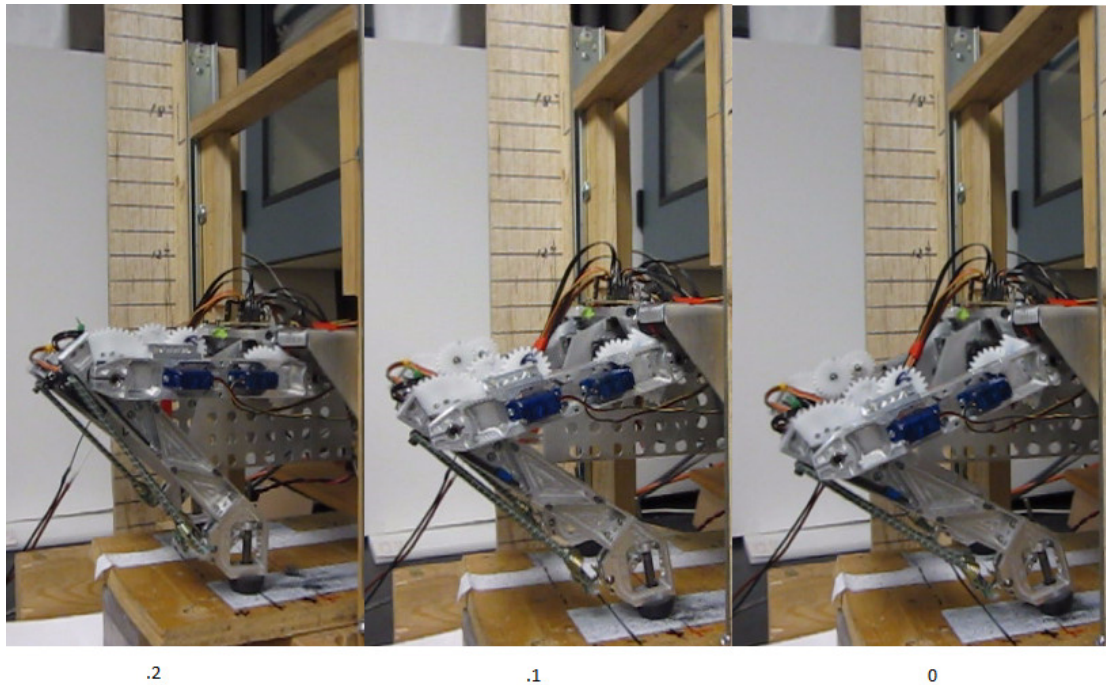
Figure 6.4 Positioning of feet

By controlling the hip angle alone, we successfully demonstrated that we could control feet landing position. We could narrow the landing spot to within a band 0.3 inches. Most of the time, the positioning stabilizes within one jump. Control of the hip angle is a PD controller of angle and angular velocity. Control input is the offset of the targeted hip angle.

6.2 Implementation of Running Gait

Running gait is essentially hopping gait with alternating foot. Implementation of running gait, however, is not as simple as one foot hopping. When one foot is compressing, the other foot must have be actuated to a sufficient height to avoid hitting the ground. Because of the soft spring chosen to maximize energy absorption, the deflection at the knee and hip is relatively big compared to that of the human's

gait. Current in the algorithm when one foot is in compress stage, the program bends the other hip forward and compresses the knee as much as possible to avoid hitting ground. Initial trial of the running gait was not successful because the motors were not powerful enough to bend the knee joints far enough.

Further tests will be conducted with modified algorithm that will bend the hips backward instead of forward.

6.3 Result of Springy Foot Test

The test produced both positive and negative results. On the positive side, the spring foot appears to absorb more energy than the previous ankle design so that the robot can hop higher. But on the other side, the foot tends to slide forward as the hopping height increases. It might due to the fact that spring tends to push the foot forward as it bounce and the pressure execrated on ground is reduced because of a wider foot surface compared to the previous design. Further testing and modifications will be needed to see how such a design might be implemented.

6.4 Discussion on the Design Shortcoming

An unexpected result of experiment was the damage on the RC servos. Figure below highlights the damage on a metal gear tooth within one of the gear train. The damage was server enough to cause the motor to occasionally seize. Even when the motor is working, its position was off compared to a normal motor.
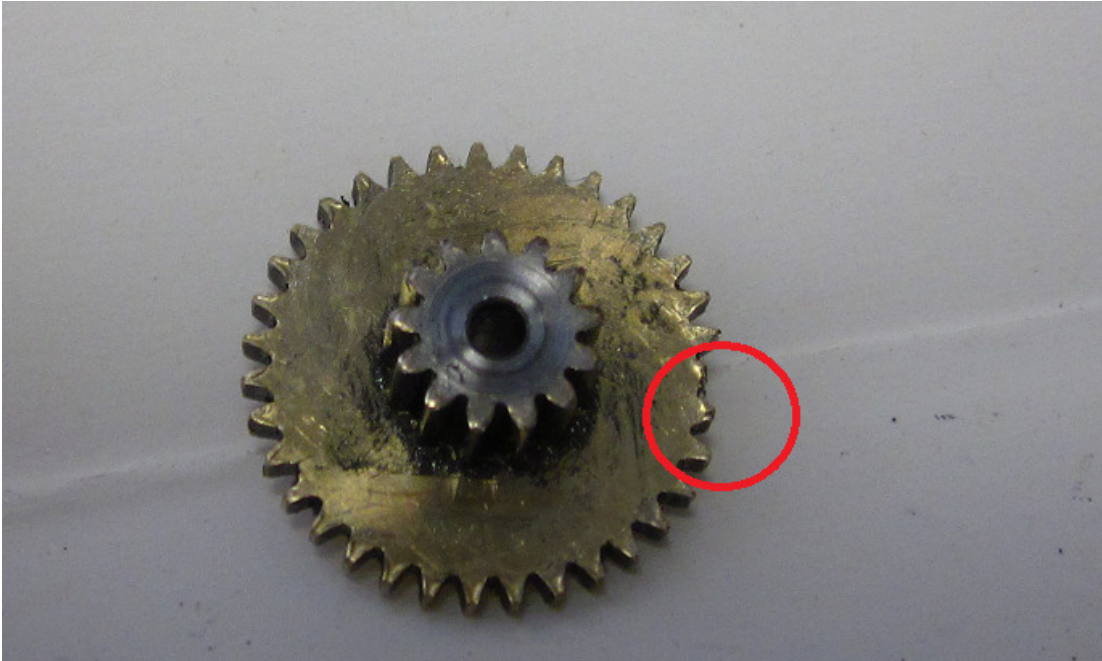
Figure 6.5 Damage on a gear of a RC servo.

Another problem surfaces at torsion spring housings. After extended testing, it is found that knee torsion spring is robbing against the housing wall. The robbing marking makes the wall rougher and might contribute the further frictional loss at joints.

The splines on the plastic horn of motor tended to wear off quickly especially during heavy testing. It is possible to replace them with metal horns which will last longer.

Previously I have mentioned that gear train backlash was found to be a major source of problem in controlling the foot positioning. There is about 2 degree of backlash at both hip and knee motors that attribute to the unstable placement of foot positioning. It's almost certain that the backlash comes from the gear train inside the RC servo because readings from potentiometers, which are connected to the joints without gears, show no sign of backlash. The problem was never resolved in this

project. Due to the fact gears need gap to move smooth, it's possible that the problem will never be resolved and the gear train has to be replaced by another mechanism.

The on-board controller of RC servo also presented a challenge. Without the knowledge of its control algorithm and a mean to reprogram it, we can only treated it as a black box and did an open loop control on the motor. When we were testing the PD controller, with a high proportional gain, the leg would start to shake violently. That limited our ability to control the hip angle. In the future, an external controller is recommended.

6.5 Conclusion

To sum up about the current state of the project,

1. We demonstrated that hopping and walking gaits are possible with current design.

2. We are able to establish control of foot landing position within 0.3".

3. Self-balancing was not implemented in current design.

4. A new drive mechanism would be needed to achieve what we set out to do.

6.6 Future work

A novel design of back drivable knee joint actuator

To over come the series of shortcoming with our current design, a design involving linkages and ball screws was identified and studied to be the best candidate for replacing the current RC servo drives.
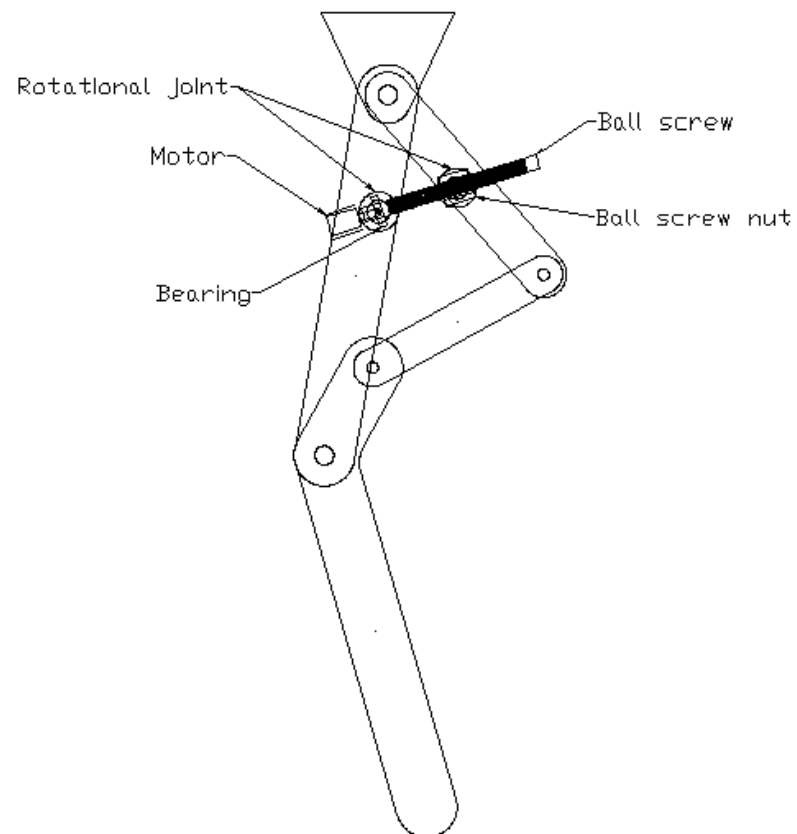
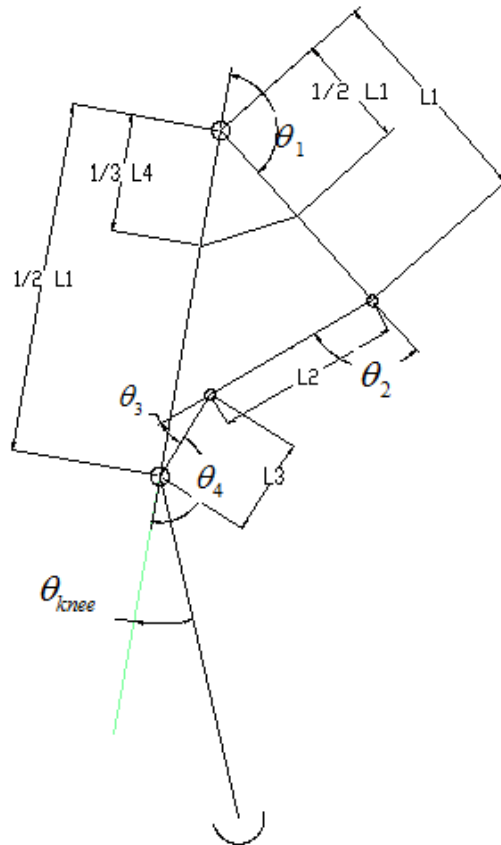**Figure 6.6 The figure illustrates the linkage design.**

Figure 6.7 This figure shows how a 4-bar linkage calculate the knee angle by controlling the ball screw lead.

Even though a ball screw assembly will be heavier than a gear train, there are several factors that lead me to believe it will beneficial to implement such a system. The primary reason for choosing ball screw, instead of a lead screw, is it's highly efficient and back drivable. According to Roton's website [8], back driving efficiency can be assumed as 80%, regardless of the lead angle, so picking a different pitch won't affect the efficiency of the power train. The efficiency is also comparable with a planetary gear system. Ball screw is also more resistant to impact.

The use of a linkage system is to achieve a variable gear ratio at different angles so that gear ratio is optimized for different tasks. For the leg design, it's ideal

to have a lower gear ratio when leg is near straight and higher gear ratio when the knee is bent. The reason is as the robot is taking off, the knee joint must move faster in order to keep pushing the leg higher, so a low gear ratio works better. But when the knee is bent, it requires more torque to start the motion while speed isn't an issue. A linkage design is shown in figure with the following configurations:

```
L1=3.9;
L2=3.2;
L3=1.75;
L4=5.6;
```

The desired kinematics of the linkage can be calculated by considering it as a 4-bar linkage system. By controlling $\Theta 1$ using a ball-screw drive, we can obtain the desired $\Theta 4$ [9]. A figure below shows the plot of gear ratio at different knee angles. With a 1mm pitch ball screw, it's possible to obtain motor to knee gear ratios ranging from 137:1 to 200:1. The output torque and speed would be close to ideal of what we hope to achieve.

We can change of parameters of the linkages to obtain a different range of gear ratios, After some trials, it was found that change of gear ratios was most sensitive to the changes of L3 link. An increase L3 will lift the profile up, as shown in the figure below. In the future, an algorithm can be devised to obtain the necessary linkage parameter to obtain the ideal range of gear ratios.
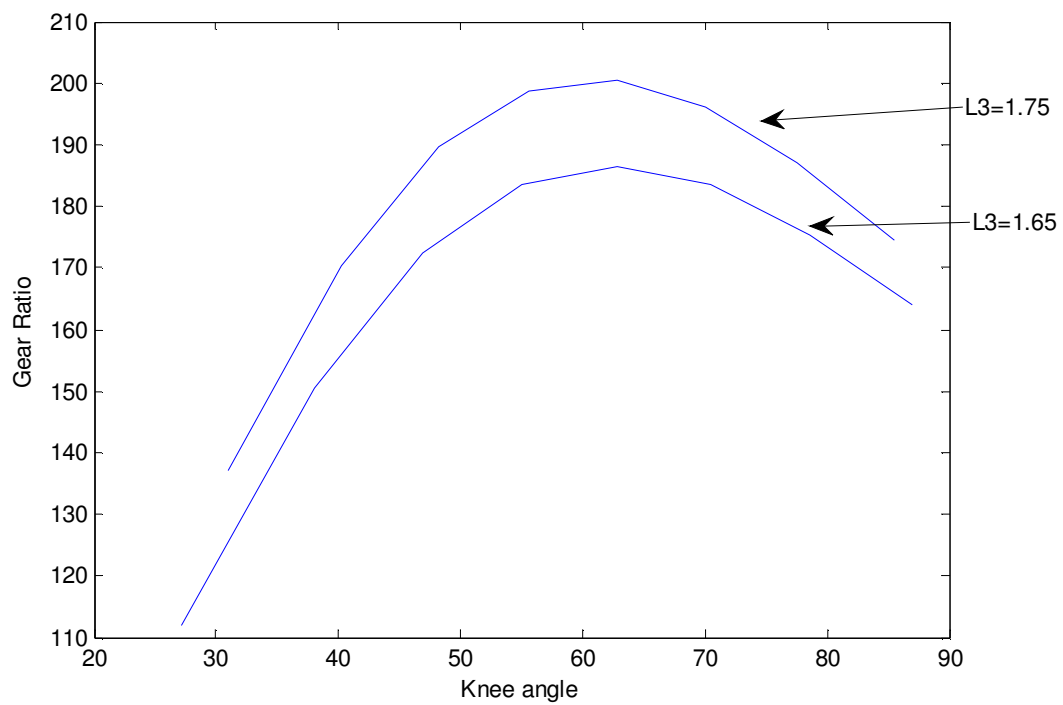
Figure 6.8 Gear ratio from motor to knee angle varies at different knee angles. A 1mm pitch ball screw is used in the calculation.

References:

1. M. H. Raibert. (1984). Hopping in legged systems modeling and simulation for the 2d one-legged case, IEEE Trans. Syst. Man Cybernet. **14**, (1984), 451–463

2. Boston Dynamics(2011) Website, Accessed July 2011at http://www.bostondynamics.com.

3. C. Semini "HyQ - design and development of a hydraulically actuated quadruped robot," Ph.D. dissertation, Italian Institute of Technology and University of Genoa, 2010

4. Ryuma Niiyama, Akihiko Nagakubo, Yasuo Kuniyoshi (2007)Mowgli: A Bipedal Jumping and Landing Robot with an Artificial Musculoskeletal System, 2007 IEEE International Conference on Robotics and Automation Roma, Italy, 10-14 April (2007), ThC5.2, 2546-2551

5. Meyer, Friedrich, Sproewitz, Alexander and Berthouze, Luc. (2006). Passive compliance for an RC servo-controlled bouncing robot. Advanced Robotics, 20, (2006), 953-961

6. H. De Man, D. Lefeber & J. Vermeulen, Design and Control of a Robot with One articulated Leg for Locomotion on irregular terrain. http://wwwtw. vub.ac.be/ond/werk/multibody.htm

7. "A Guide to Using RC Airplane Servos", http://www-cdr.stanford.edu/dynamic/servo/. Standford, Web. 13 Jul 2011. <", http://www-cdr.stanford.edu/dynamic/servo/>

8. "Application Engineering." *http://www.roton.com*. Roton Products, Inc., n.d. Web. 13 Jul 2011. <http://www.roton.com/application_engineering.aspx#7>.

9. LaValle, Steven M. *Planning Algorithms*. Cambridge: Cambridge University Press, 2006. 101-105. Print.

Appendix 1 Bill of Materials

The following table includes the major *off-the-shelves* parts used to in this prototype robot. It does not include fasteners (screws, dowels), minor electronic components, and other miscellaneous hardware.

Table A.1: Bill of Materials of off-the-shelves components

Part	Manufacturer/Vendor	Vendor Part Number	QTY
Digital servo DS120M	Pololu.com	1052	4
Analog servo Hitec HS-55	towerhobbies	LXTX42	4
Torsion spring, hip(left)	Mcmaster	9271K66(left)	1
Torsion spring, hip(right)	Mcmaster	9271K65(right)	1
Torsion spring, knee(left)	Mcmaster	9271K72-L	1
Torsion spring, knee(right)	Mcmaster	9271K72-R	1
Ball bearing	Mcmaster	57155K375	8
Microprocessor		sbRIO	1